

A METHOD OF DESIGNING MAGNETIC CHANNELS OF IMPROVED FIELD QUALITY FOR SUPERCONDUCTING CYCLOTRONS

P. R. Sarma, V. S. Pandit and R. K. Bhandari

Variable Energy Cyclotron Centre, Bidhannagar, Kolkata-700 064, India

Abstract

Magnetic channels are used in the extraction system of superconducting cyclotrons for focusing and extracting the high energy beam. In order to preserve the beam quality, the field gradient produced by the channels should be constant. We have evolved a procedure based on the linear programming technique for optimizing the geometry of magnetic channels. With this, we have reduced the deviation in the field gradient not only in the median plane but through the beam aperture.

1 INTRODUCTION

In high energy cyclotrons, especially in superconducting cyclotrons, in addition to electrostatic deflectors, passive magnetic channels are used for extracting the beam. These channels use iron bars to lower the magnetic field in the extraction region thereby helping the extraction process. These also generate a positive field gradient (opposite to radially defocusing fringe field gradient) and so provide a radial focusing force. At Variable Energy Cyclotron Centre in Calcutta, a K500 superconducting cyclotron, similar to the one at Michigan State University[1], is under construction. The extraction system uses 9 magnetic channels[2].

Typical magnetic channels consist of three iron bars, one placed at a lower radius and two other at a higher radius with respect to a beam orbit (Fig. 1)[3]. In the strong field of the superconducting cyclotron these bars become magnetically saturated. The single bar on the left reduces the field near it and the other two bars on the right increase the field at higher radii. The combined effect is a negative field in the centre of the channel and a radially focusing gradient within the aperture occupied by the beam. Such magnetic channels have been used in the superconducting cyclotrons at Chalk-River[4], NSCL at MSU[5] and at Milan[6].

In order to preserve the beam quality, it is necessary that the field gradient of the channel be constant along the radial direction not only in the median plane but also in the planes above and below it, because the beam has finite radial and vertical dimensions. The field gradient is determined by the dimensional parameters of the channel geometry. Recently we developed a method[7], based on the linear programming technique, to optimize the channel parameters for reducing the deviations of the field gradient. We considered only purely rectangular bar shapes there. Here we have improved and used the method to further improve the field quality of the channel by considering other shapes.

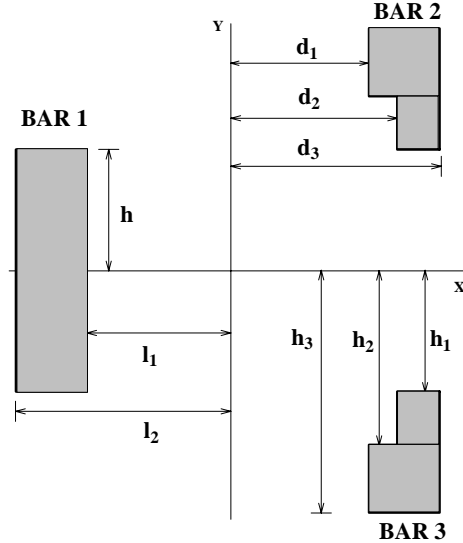


Figure 1: Channel geometry showing various dimensional parameters.

2 CALCULATION OF MAGNETIC FIELD

Since the iron bars are completely saturated, the field due to the bars is the same as that due to current sheets on the vertical surfaces of the bars. Thus $B_z(x, y)$, the vertical component of the field at a point (x, y) due to a bar of thickness t and height $2h$, placed at a distance d from the origin is

$$B_z(x, y) = A \left[\int_{-h-y}^{h-y} \frac{(d-x)}{(d-x)^2 + y^2} dy - \int_{-h-y}^{h-y} \frac{(d+t-x)}{(d+t-x)^2 + y^2} dy \right] \quad (1)$$

where $A = -3.375$ kG in the case of iron saturated to 21.4 kG. This can be simplified to

$$B_z(x, y) = A \left[\tan^{-1} \frac{h-y}{d-x} - \tan^{-1} \frac{h-y}{d+t-x} + \tan^{-1} \frac{h+y}{d-x} - \tan^{-1} \frac{h+y}{d+t-x} \right] \quad (2)$$

One can add the field contribution by the three bars (Fig. 1) to get the total field as

$$B_z(x, y) = A \left[\tan^{-1} \frac{h_3-y}{d_1-x} - \tan^{-1} \frac{h_1-y}{d_1-x} - \right]$$

$$\begin{aligned}
& \tan^{-1} \frac{h_3 - y}{d_3 - x} + \tan^{-1} \frac{h_1 - y}{d_3 - x} + \tan^{-1} \frac{h_3 + y}{d_1 - x} - \\
& \tan^{-1} \frac{h_1 + y}{d_1 - x} - \tan^{-1} \frac{h_3 + y}{d_3 - x} + \tan^{-1} \frac{h_1 + y}{d_3 - x} - \\
& \tan^{-1} \frac{h_2 - y}{d_1 - x} - \tan^{-1} \frac{h_1 - y}{d_1 - x} - \tan^{-1} \frac{h_2 - y}{d_2 - x} + \\
& \tan^{-1} \frac{h_1 - y}{d_2 - x} - \tan^{-1} \frac{h_2 + y}{d_1 - x} - \tan^{-1} \frac{h_1 + y}{d_1 - x} - \\
& \tan^{-1} \frac{h_2 + y}{d_2 - x} + \tan^{-1} \frac{h_1 + y}{d_2 - x} + \tan^{-1} \frac{h - y}{l_1 + x} - \\
& \tan^{-1} \frac{h - y}{l_2 + x} + \tan^{-1} \frac{h + y}{l_1 + x} - \tan^{-1} \frac{h + y}{l_2 + x} \Big] \quad (3)
\end{aligned}$$

We want that the field due to the channel should have a specific value $B(0,0)$ at the chosen centre and have a chosen field gradient G , i.e.,

$$B_z(x, y) = B(0, 0) + Gx \quad (4)$$

for all y . The actual field of the channel will somewhat deviate from this and our endeavour is to minimize the deviation by optimizing the channel geometry.

3 LINEAR PROGRAMMING METHOD

The parameters which have been optimized are $h, h_1, h_2, h_3, d_1, d_2$ and d_3 . As seen from eqn.(3), $B_z(x, y)$ is not a linear function of these parameters and so is not directly amenable to linear programming. So we first linearize the field in a small range. In the neighbourhood of any set of the parameters we can expand the function $B_z(x, y)$ to get

$$\begin{aligned}
B_z(x, y) &= B_{z0}(x, y) + \Delta h \left(\frac{\partial B_z}{\partial h} \right)_0 \\
&+ \Delta h_1 \left(\frac{\partial B_z}{\partial h_1} \right)_0 + \Delta h_2 \left(\frac{\partial B_z}{\partial h_2} \right)_0 + \Delta h_3 \left(\frac{\partial B_z}{\partial h_3} \right)_0 \\
&+ \Delta d_1 \left(\frac{\partial B_z}{\partial d_1} \right)_0 + \Delta d_2 \left(\frac{\partial B_z}{\partial d_2} \right)_0 + \Delta d_3 \left(\frac{\partial B_z}{\partial d_3} \right)_0 \quad (5)
\end{aligned}$$

where $B_{z0}(x, y)$ is the field at (x, y) with the initial set of parameters. This is linear in terms of the increments $\Delta h, \Delta h_1$ etc. and so one can now apply linear programming to minimize $|B_z(x, y) - B(0, 0) - Gx|$. We use the constraint that the deviations from the design field profile should be smaller than the tolerance for $-x_m \leq x \leq x_m$ where $2x_m$ is the maximum beam width in the horizontal plane. The constraint is used at another parallel plane also with $y = y_m$ where $2y_m$ is the vertical width of the beam. We have taken $x_m = 0.3$ cm and $y_m = 0.2$ cm. This is done at a number of points, x_1, x_2, \dots within $-x_m$ to x_m to get the set of constraints as

$$B_z(x_1, 0) - B(0, 0) - Gx_1 < Tolerance$$

$$B_z(x_2, 0) - B(0, 0) - Gx_2 < Tolerance$$

.....

$$B_z(x_1, y_m) - B(0, 0) - Gx_1 < Tolerance$$

.....

(6)

Since $[B_z(x, y) - B(0, 0) - Gx]$ can be either positive or negative, we have to use another set of constraints

$$-B_z(x_1, 0) + B(0, 0) + Gx_1 < Tolerance$$

.....

(7)

We have also put restrictions to the ranges within which the parameters are allowed to vary. The simplex technique is used for solving this problem of for minimizing *Tolerance*. The standard simplex technique maximizes the value of a variable. Since we want to minimize a variable, we do it by introducing a variable *Tol* given by

$$Tolerance = Tolmax - Tol$$

where *Tolmax* is an arbitrarily large constant. *Tol* can now be maximized for minimizing *Tolerance*. The simplex algorithm gives a set of corrections $\Delta h, \Delta h_1$ etc. We do the calculation in an iterative manner, in which a small fraction of the correction is applied at each step. It is necessary to specify whether one wants to increase or decrease any particular parameter. If in any trial a parameter remains unchanged, its sign is reversed in the next trial.

4 RESULTS AND DISCUSSION

We started with the geometry of the channel used in K500 machine at MSU[6] (Table 1). It has $B(0, 0) = -1.214$ kG and $G(0, 0) = 3.3$ kG/cm. Fig. 2 shows the geometry of the optimized channel. The dotted geometry is that of the unoptimized one. We have not tried to change the parameters l_1 and l_2 of Bar 1 as these will change the field appreciably inside the cyclotron. However, the other six parameters have little influence on the field on the left of Bar 1 and have been optimized.

Fig. 3(a) compares the deviation of the field from the design field profile. Fig. 3(b) shows that the deviation in gradient as a function of x . The deviation in the optimized channel comes down to 0.20 kG/cm from 0.83 kG/cm in the unoptimized channel. The superiority of the optimized channel is obvious. The optimization also decreases the values of the unwanted higher harmonic field components, responsible for the nonlinear effects. The optimized geometry gives a variation of 2.6 kG/cm² in the sextupolar component compared to 9.1 kG/cm² in the unoptimized geometry (Fig. 3(c)).

Fig. 4 compares the estimated beam ellipses when a beam of emittance of 9 mm.mrad passes through the 9 optimized and unoptimized channels. The ellipse gets distorted appreciably by the unoptimized channels and the overall emittance increases by about 30%.

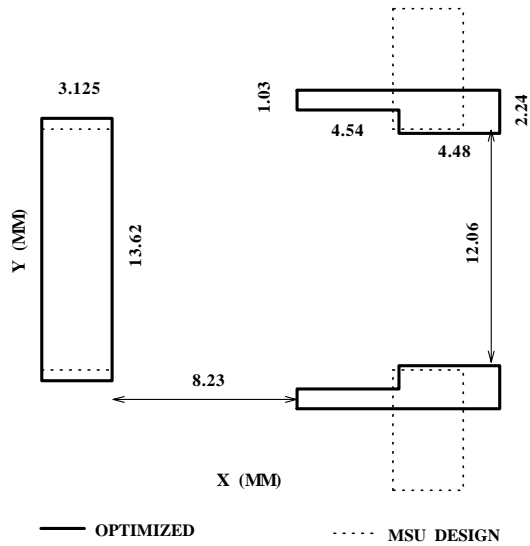


Figure 2: Optimized channel geometry compared with the MSU channel.

Table 1: Channel dimensions and field quality

Parameter	Unoptimized	Optimized
h (cm)	0.625	0.681
h_1 (cm)	0.625	0.603
h_2 (cm)	0.625	0.724
h_3 (cm)	1.25	0.827
d_1 (cm)	0.625	0.198
d_2 (cm)	0.625	0.652
d_3 (cm)	0.9375	1.10
l_1 (cm)	0.625	0.625
l_2 (cm)	0.9375	0.9375
Max. ΔG (kG/cm)	0.840	0.206

The present method can be applied to other simple geometries also, e.g., in a channel which only lowers the field but does not produce any gradient or a channel of any required field profile.

5 ACKNOWLEDGEMENT

We thank Mr. M.K. Dey for his help in computing the beam ellipses.

6 REFERENCES

- [1] R.K. Bhandari, Proceedings of the 15th. International Conference on Cyclotrons and their Applications, Caen, 1998, p.692.
- [2] E. Fabrici, D. Johnson and F.G. Resmini, Nuclear Instruments and Methods /bf 184(1981)301.
- [3] M. Odera, Y. Miyazawa, T. Tonuma, M. Hemmi and O. Terajima, Nuclear Instruments and Methods **65**(1968)247.
- [4] C.R. Hoffman, IEEE Trans. on Nuclear Science, NS-24(1977)1470.

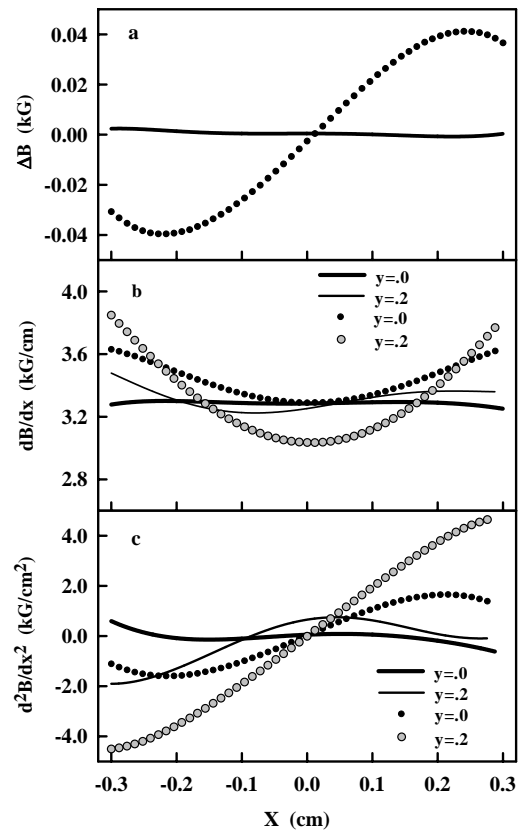


Figure 3: Comparison of the deviations in the (a) field, (b) field gradient, and (c) second gradient of the field. The solid curves are for the optimized channel and the dotted curves are for the unoptimized channel.

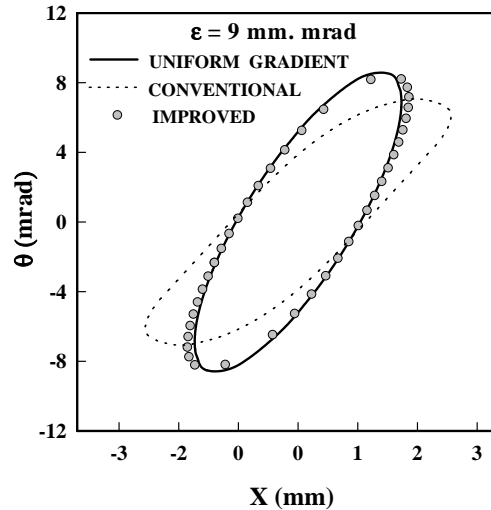


Figure 4: Comparison of beam ellipses as the exit of the 9 optimized and unoptimized channels.

- [5] M.M. Gordon, D.A. Johnson and V. Taivassalo, MSU Cyclotron Laboratory Annual Report (1983-84), p.218.
- [6] G. Bellomo, Proceedings of the 13th International Conference on Cyclotrons and their Applications, Vancouver, 1992, p.592.
- [7] P.R. Sarma, V.S. Pandit and R.K. Bhandari, Nuclear Instruments and Methods **455**(2000)539.